

# Properties of $^{156}\text{Gd}$ levels populated in the decay of 15.2 day $^{156}\text{Eu}$

A. F. Kluk\* and Noah R. Johnson

*Oak Ridge National Laboratory,† Oak Ridge, Tennessee 37830*

J. H. Hamilton

*Physics Department, Vanderbilt University,‡ Nashville, Tennessee 37203*

(Received 20 March 1974)

$\gamma$  rays emitted in the radioactive decay of 15.2 day  $^{156}\text{Eu}$  have been studied with large volume Ge(Li) detectors in both singles and coincidence modes. A total of 95  $\gamma$ -ray transitions were observed in the  $^{156}\text{Eu}$  decay and 84 of these are placed in the  $^{156}\text{Gd}$  level scheme which consists of 26 excited states. Seven of these levels are assigned here for the first time. Many of the inconsistencies that have complicated the interpretation of previous work have been resolved in these studies. In particular, it has been possible in the extensive coincidence measurements to resolve several multiplets in the  $\gamma$ -ray spectrum and, therefore, to obtain accurate branching intensities for members of both the  $\gamma$ -vibrational band and two  $K^\pi = 0^+$  excited bands.

[ RADIOACTIVITY  $^{156}\text{Eu}$  (from  $n$  capture on  $^{154}\text{Sm}$ ); measured  $E_\gamma$ ,  $I_\gamma$ ,  $\gamma$ - $\gamma$  coin; deduced  $\log ft$ .  $^{156}\text{Gd}$  deduced levels,  $J$ ,  $\pi$ , ICC. Enriched  $^{154}\text{Sm}$  target, Ge(Li) detectors. ]

## I. INTRODUCTION

Because of the unexpected behavior found<sup>1-7</sup> for the decay patterns of the vibrational states in  $^{152}\text{Sm}$  and  $^{154}\text{Gd}$ , it seemed important to extend the information on the level properties of  $^{156}\text{Gd}$  which is expected to display more typical rotational behavior. Accordingly, a few years ago we began such studies using radioactive sources of  $^{156}\text{Eu}$ .

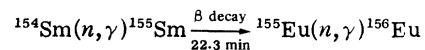
At the time the present work was initiated there was a very limited amount of high resolution data available on the decay of  $^{156}\text{Eu}$ . These included the internal-conversion electron measurements of Ewan, Graham, and Geiger<sup>8</sup> and Peek, Jungerman, and Patten<sup>9</sup> and some preliminary measurements with Ge(Li) detectors by Ewan and Bower.<sup>10</sup> More recently NaI-Ge(Li) directional correlation measurements have been done by Hamilton *et al.*<sup>11</sup> and Rud and Nielsen.<sup>12</sup> Higher spin states of  $^{156}\text{Gd}$  have been studied through neutron-capture experiments<sup>13-17</sup> and from the decay<sup>18-21</sup> of  $^{156}\text{Tb}$  which has a ground-state spin of  $3^-$ . Additional experiments done on the properties of collective levels in  $^{156}\text{Gd}$  include ( $d, d'$ ) inelastic scattering,<sup>22</sup> ( $\alpha, xn$ ) reactions,<sup>23</sup> and Coulomb excitation studies.<sup>24, 25</sup>

The measurements in the present study were performed with large-volume high resolution Ge(Li) detectors. Both singles and extensive  $\gamma$ - $\gamma$  coincidence experiments were performed and from these we have been able to assign 26 excited states in  $^{156}\text{Gd}$  with 7 of these reported for the first time. Of the 95  $\gamma$ -ray transitions measured here, 84 are placed in this level scheme. In addition, many of the inconsistencies that complicated the interpreta-

tion of previous works have been resolved. In particular, it has been possible in the coincidence measurements to resolve several multiplets in the  $\gamma$ -ray spectrum and, therefore, to obtain accurate branching intensities for members of both the  $\gamma$ -vibrational band and two  $K^\pi = 0^+$  excited bands. In a recent paper<sup>26</sup> we made a comparison of these branching ratios with the rotational model predictions modified by a second-order perturbational calculation.

## II. EXPERIMENTAL APPARATUS AND PROCEDURES

The 15 day  $^{156}\text{Eu}$  activity was prepared in the Oak Ridge research reactor by irradiation of 10 mg samples of  $\text{Sm}_2\text{O}_3$  which was 99.54% enriched in  $^{154}\text{Sm}$  by the Oak Ridge Isotopes Division. The double neutron-capture process



was utilized. Following a 5 day irradiation, the source was dissolved in concentrated hydrochloric acid and an ion-exchange chemical purification was performed. Sources for  $\gamma$ -ray analyses were prepared by evaporating a drop of the purified europium chloride to dryness on a Mylar source mount. One half-life after irradiation about 6% of the source activity was due to 1.8-yr  $^{155}\text{Eu}$ . However, since the  $^{155}\text{Eu}$   $\gamma$  rays are all of low energy (the available decay energy is 248 keV), they did not hinder the  $^{156}\text{Eu}$  measurements. Due to the shorter half-life, the  $^{156}\text{Eu}$  peaks were easily identified by following the decay of the source.

For the  $\gamma$ -ray singles measurements we used a 40-cm<sup>3</sup> coaxial Ge(Li) detector with an efficiency of 6.5%. The system resolution at a count rate of 1000 counts per second was 2.1 keV full width at half-maximum (FWHM) for the 1333-keV  $\gamma$  ray of <sup>60</sup>Co. Coincidence experiments were performed with two large-volume Ge(Li) detectors coupled to a 4096  $\times$  4096 two-parameter analyzer. The two germanium diodes were located at 90° to one another and were shielded by a lead baffle to minimize detector-to-detector Compton scattering. Gating pulses were generated with a time-to-amplitude converter (TAC) for which constant fraction timing units provided the start and stop pulses. The resolution ( $2\tau$ ) of the pulse distribution from the TAC was 25 nsec. A pile-up rejection system consisting of an integral discriminator, a pile-up rejector, delay amplifier, and linear gate was operated between the first and second amplification of each TC-200 amplifier.

The maximum accumulation rate for coincidence data in this experiment was about 100 events per second. Each coincidence event was stored on magnetic tape as an element ( $X_i, Y_i$ ) of a 4096  $\times$  4096 array. A total of six magnetic tapes containing about  $2 \times 10^6$  events each were accumulated and processed. A computer program was developed to sort the data into spectra, each of which was coincident with a particular region of interest called a coincidence window or "gate" in the spectrum of one of the detectors. Coincidence windows were set on all full-energy peaks of interest and

on the background just above or below the full-energy peaks to account for events that are coincident with the Compton background. Corrections were made for the chance contributions which were negligible in most cases.

During the coincidence measurements, singles spectra were sampled for 1% of the clock time and stored in two 2048-channel blocks of the hard wired memory. At preselected time intervals these singles were automatically transferred to magnetic tape.

Absolute efficiency curves for the Ge(Li) detectors were determined from several calibrated sources. Errors in the absolute efficiencies were estimated to be less than 5% in the range of 200–3200 keV and less than 10% in the range of 50–200 keV. Errors in the relative efficiencies over the entire energy range are probably less than 5% but we used this upper limit in the estimates of all errors in relative intensities.

### III. SINGLES $\gamma$ -RAY RESULTS

Typical  $\gamma$ -ray singles spectra obtained for <sup>156</sup>Eu decay are shown in Figs. 1 and 2. These spectra represent the channel by channel summation of four runs taken consecutively on a single source over a 66-h period. Counting rates ranged from 1000 to 1500 per second. The spectrum below 60 keV is not included in Fig. 1, but it contains a complex of x rays and <sup>155</sup>Eu impurity peaks. The effective resolution of the prominent 1277.4-keV peak in Fig. 1 is  $\sim 2.4$  keV due to small drifts in

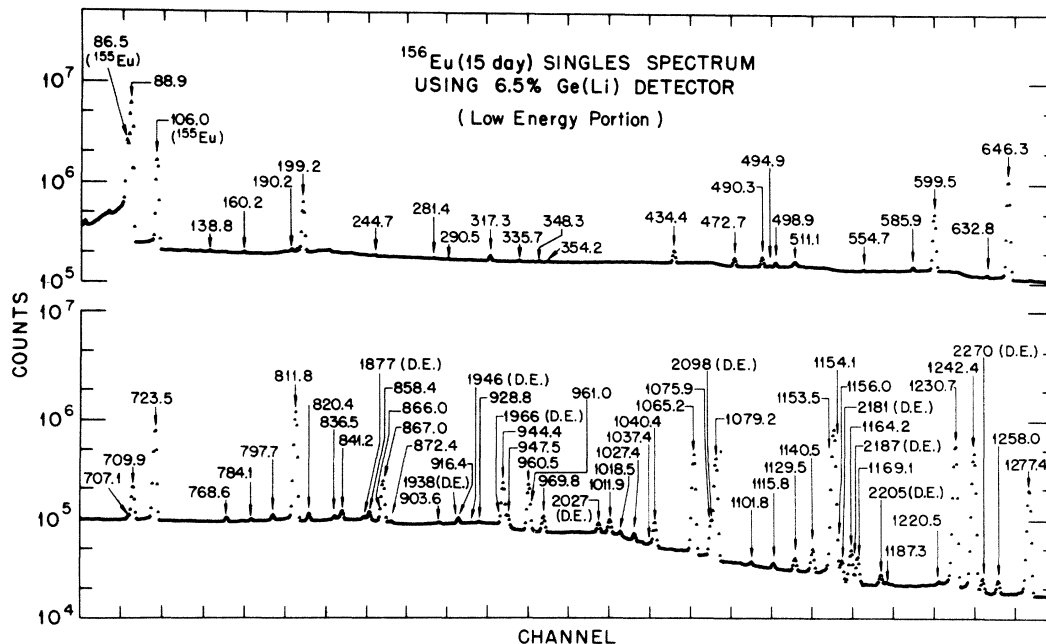


FIG. 1. Low-energy section of <sup>156</sup>Eu singles spectrum taken with a large-volume Ge(Li) detector.

the system gain during the course of the measurements.

The energies of the most intense peaks in the  $^{156}\text{Eu}$  spectrum were measured by counting  $^{156}\text{Eu}$  sources simultaneously with several energy-standard sources. Once these more prominent peak energies were obtained, they were used as internal standards to determine the energies of the weaker peaks.

Peak positions of the  $\gamma$  rays were obtained with a computer program which used a three-parameter linear least-squares fitting procedure to fit a Gaussian curve to the data points of the photopeak corrected for background. In most cases the background was determined from a linear fit to the data points on either side of the peak.

The energy calibration was determined by a least-squares fit of an  $n$ th degree polynomial to the  $\gamma$  rays from several standard sources. For this fit, the peak positions were corrected for spectrometer nonlinearity as measured with a precision pulser. The nonlinearity correction was  $\leq(\pm 0.55)$  channels over 95% of the analog-to-digital converter (ADC) range. The error in the linearity correction was estimated to be between 0.05 and 0.1 channels and was folded into the peak-position error. A third degree polynomial was found to give the best fit.

The energies of the transitions observed in the decay of  $^{156}\text{Eu}$  are listed in Table I. Errors assigned to these energies range from 50 eV for the most intense  $\gamma$ -ray transitions measured by the standards-in-place technique, to 0.7 keV for weak high-energy transitions.

Relative intensities of the  $\gamma$  rays were obtained from the peak areas determined both from the area of a computer-fitted Gaussian curve and from a channel-by-channel summation of the counts in the peak. These two methods of area measurement agreed within the assigned errors in most cases except for very weak peaks where the Gaussian fit was obviously poor. Therefore, channel-by-channel summation was used for the listed relative intensities of the very weak peaks. As seen in Table I, errors in the relative intensities ranged from 5% for the most intense  $\gamma$  ray to about 50% for the weak ones.

#### IV. $\gamma$ - $\gamma$ COINCIDENCE RESULTS

A summary of the results of the  $\gamma$ - $\gamma$  coincidence experiments is given in Table II. Coincidence gates for all the prominent  $\gamma$  rays which are necessary to establish the features of the level scheme are listed in the first row. The observation of a  $\gamma$  ray in the spectrum coincident with a gating  $\gamma$  ray

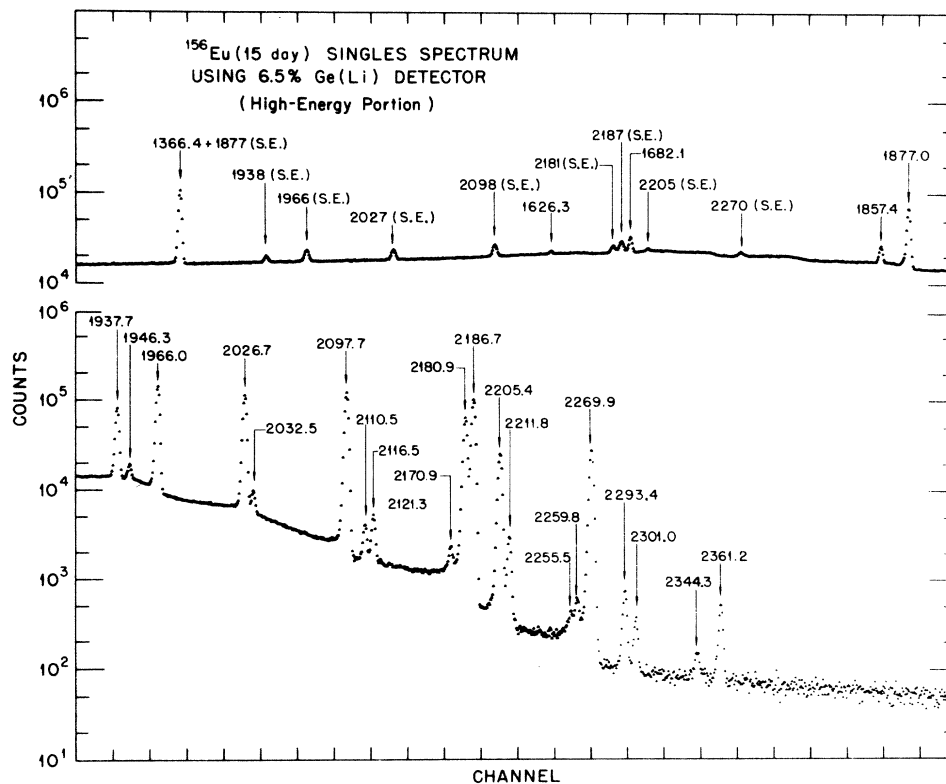


FIG. 2. High-energy section of  $^{156}\text{Eu}$  singles spectrum taken with a large-volume Ge(Li) detector.

is indicated in the table by one of the following entries: VS, S, W, VW, P. They represent very strong, strong, weak, very weak and probable, respectively. These entries represent the strength of the observed  $\gamma$  ray relative to the other  $\gamma$  rays in the coincidence spectrum. The last entry represents a coincidence relationship which within the error limits of the coincidence data is probable, yet not conclusive.

It is impractical to discuss in detail the extensive data of Table II. Instead, we will cover only a few pertinent situations and, likewise, show only a few coincidence spectra which illustrate the utility of these data in deducing the intricate details of the level scheme shown in Fig. 3.

In the decay of  $^{156}\text{Eu}$  there are several complex peaks (e.g., those at 867, 1079, and 1154 keV) which could only be resolved with the aid of the coincidence data. We were able to see that there was an 1153-1154-keV doublet by setting gates on the high and low side of the peak as shown in Figs. 4(b) and 4(c), respectively. But to completely resolve this doublet, it was necessary to use the spectrum coincident with the 811.77-keV transition [see Fig. 5(b)] which directly populates the 1154.09-keV state in the  $^{156}\text{Gd}$  level scheme of Fig. 3. In this coincidence spectrum the 88.95-, 199.19-, 866.0-, 1065.14-, and 1154.09-keV  $\gamma$  rays can be seen where the latter three transitions depopulate the  $2^+$  level of the  $\gamma$ -vibrational band.

TABLE I. Energies and relative intensities of  $\gamma$  rays observed in the decay of  $^{156}\text{Eu}$ .

$\gamma$ -ray energy (keV)	Relative intensity	$\gamma$ -ray energy (keV)	Relative intensity	$\gamma$ -ray energy (keV)	Relative intensity
88.95 ± 0.05 <sup>a</sup>	87 ± 9	836.52 ± 0.07	0.86 ± 0.11	1169.12 ± 0.05 <sup>e</sup>	2.82 ± 0.20
138.7 ± 0.2	0.081 ± 0.009	839.0 ± 0.2	0.32 ± 0.08	1187.3 ± 0.5	0.15 ± 0.07
160.2 ± 0.2	0.106 ± 0.011	841.16 ± 0.10	2.33 ± 0.16	1220.50 ± 0.11	0.17 ± 0.06
190.16 ± 0.08	0.170 ± 0.016	858.36 ± 0.12	1.21 ± 0.12	1230.71 ± 0.06	83.8 ± 4.2
199.19 ± 0.05	7.6 ± 0.4	865.98 ± 0.12 <sup>a</sup>	1.53 ± 0.30	1242.42 ± 0.05	69.1 ± 3.4
215.7 ± 0.2	0.13 ± 0.03	867.01 ± 0.08	13.5 ± 1.4	1258.03 ± 0.07	0.95 ± 0.09
244.7 ± 0.3	0.09 ± 0.03	872.39 ± 0.09	0.32 ± 0.07	1277.43 ± 0.05	30.3 ± 1.5
281.4 ± 0.2	0.08 ± 0.02	903.62 ± 0.10	0.31 ± 0.08	1366.41 ± 0.05	17.0 ± 0.9
290.49 ± 0.15	0.09 ± 0.02	916.4 ± 0.4	0.40 ± 0.20	1626.29 ± 0.14	0.34 ± 0.07
317.30 ± 0.09	0.65 ± 0.04	928.8 ± 0.4	0.24 ± 0.08	1682.10 ± 0.12	2.76 ± 0.20
335.69 ± 0.11	0.105 ± 0.014	944.35 ± 0.07	13.4 ± 0.8	1857.42 ± 0.11	2.45 ± 0.17
348.27 ± 0.09	0.14 ± 0.02	947.46 ± 0.15	3.0 ± 0.9	1877.03 ± 0.15	16.2 ± 0.8
354.20 ± 0.09	0.15 ± 0.02	960.50 ± 0.08	14.9 ± 1.3	1937.71 ± 0.11	20.1 ± 1.0
434.40 ± 0.09	2.12 ± 0.11	961.0 ± 0.6 <sup>b</sup>	1.5 ± 0.3 <sup>c</sup>	1946.34 ± 0.13	1.82 ± 0.13
472.70 ± 0.06	1.41 ± 0.08	969.83 ± 0.06	3.72 ± 0.18	1965.95 ± 0.12	40.2 ± 2.1
490.34 ± 0.06	1.75 ± 0.12	1011.87 ± 0.05	3.27 ± 0.20	2026.65 ± 0.11	33.9 ± 1.7
494.90 ± 0.15	0.16 ± 0.07	1018.50 ± 0.10	0.78 ± 0.09	2032.51 ± 0.12	1.25 ± 0.11
498.88 ± 0.06	0.60 ± 0.07	1027.39 ± 0.08	1.15 ± 0.10	2097.70 ± 0.11	39.8 ± 2.0
554.66 ± 0.06	0.23 ± 0.05	1037.43 ± 0.43 <sup>a</sup>	0.34 ± 0.06 <sup>d</sup>	2110.52 ± 0.13	0.82 ± 0.08
585.90 ± 0.06	0.65 ± 0.06	1040.44 ± 0.07	5.1 ± 0.3	2116.49 ± 0.13	1.21 ± 0.08
599.47 ± 0.05	21.7 ± 1.1	1065.14 ± 0.05	50.3 ± 2.5	2121.3 ± 0.4	0.048 ± 0.016
632.79 ± 0.08	0.36 ± 0.06	1075.99 ± 0.20 <sup>a</sup>	3.6 ± 0.6 <sup>c</sup>	2170.86 ± 0.20	0.53 ± 0.05
646.29 ± 0.05	65.0 ± 3.3	1079.16 ± 0.05	42.3 ± 2.5	2180.91 ± 0.12	23.3 ± 1.2
701.1 ± 0.2	0.42 ± 0.14	1101.80 ± 0.11	0.36 ± 0.11	2186.71 ± 0.11	35.3 ± 1.8
709.86 ± 0.05	8.8 ± 0.5	1115.78 ± 0.07	0.55 ± 0.08	2205.38 ± 0.13	9.2 ± 0.5
723.47 ± 0.05	55.8 ± 2.8	1129.47 ± 0.07	1.39 ± 0.12	2211.83 ± 0.12	0.93 ± 0.06
768.56 ± 0.07	0.86 ± 0.09	1140.51 ± 0.05	2.85 ± 0.19	2255.5 ± 0.5	0.062 ± 0.012
784.14 ± 0.10	0.40 ± 0.07	1153.47 ± 0.07 <sup>a</sup>	68.6 ± 6.7 <sup>c</sup>	2259.8 ± 0.3	0.171 ± 0.017
797.73 ± 0.06	1.06 ± 0.13	1154.09 ± 0.07 <sup>a</sup>	50.6 ± 4.5 <sup>c</sup>	2269.90 ± 0.12	10.6 ± 0.53
811.77 ± 0.05	100	1155.95 ± 0.3 <sup>a</sup>	1.35 ± 0.20 <sup>c</sup>	2293.40 ± 0.12	0.24 ± 0.02
820.36 ± 0.07	1.54 ± 0.10	1164.2 ± 0.3 <sup>b</sup>	0.58 ± 0.09	2301.0 ± 0.2	0.096 ± 0.016
				2344.3 ± 0.7	0.025 ± 0.006
				2361.2 ± 0.3	0.177 ± 0.017

<sup>a</sup> The energy was deduced from energy sums or differences.

<sup>b</sup> The energy was deduced from the coincidence data.

<sup>c</sup> The relative intensity was obtained from the coincidence analysis.

<sup>d</sup> The relative intensity was obtained from a linear plot by summing the counts under the peak.

<sup>e</sup> This peak was obscured in the singles by a double escape peak.

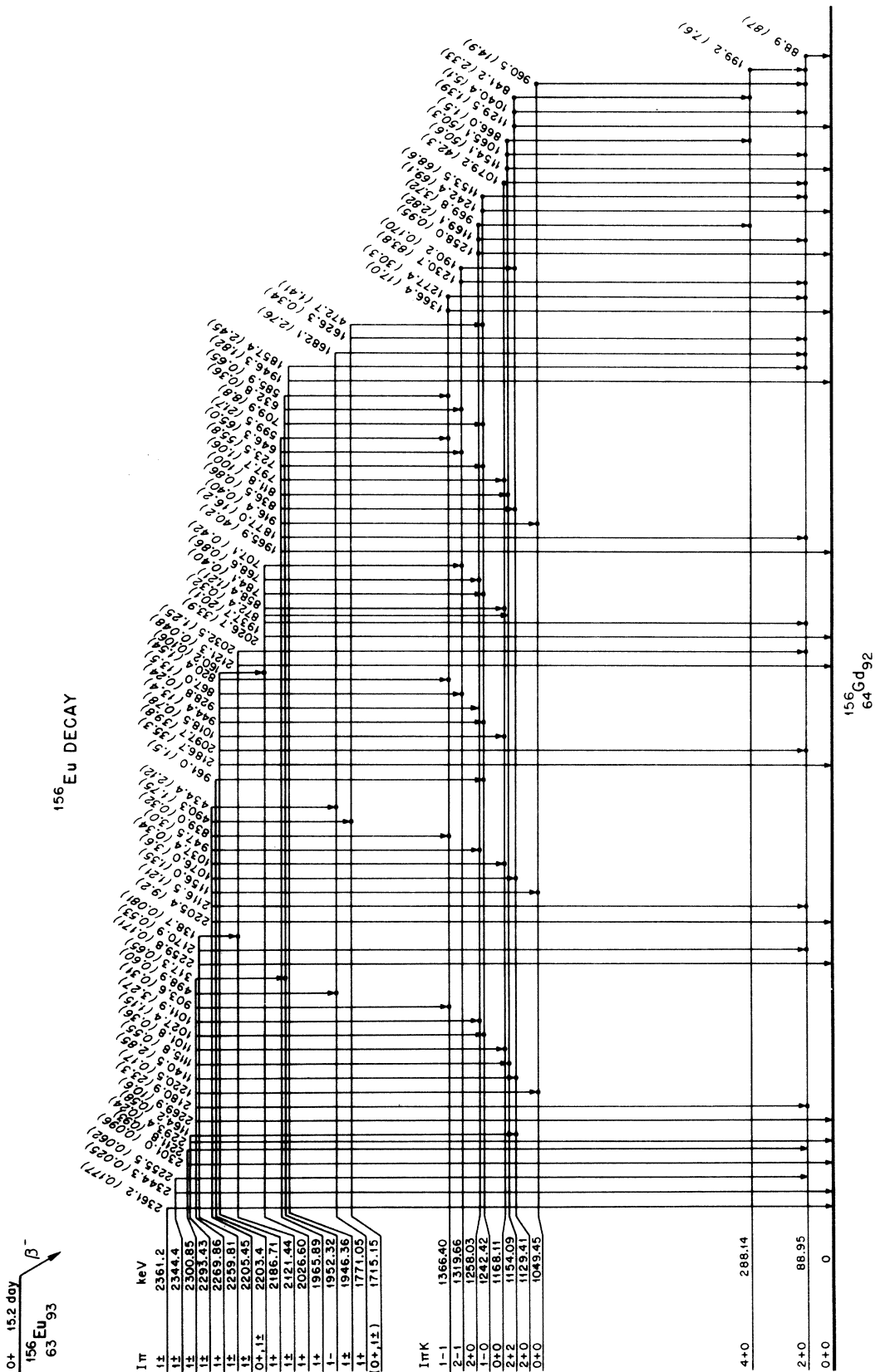


FIG. 3. Level scheme of <sup>156</sup>Gd populated in the decay of <sup>156</sup>Eu. Transitions which were shown by the coincidence data to populate an excited level are indicated by a dot at the tip of the arrow, while those which were observed in a coincidence relationship as transitions which deexcite a level are indicated by a dot at the top of the arrow. The spin (*I*) and parity ( $\pi$ ) of each level is listed in the left column; the quantum number *K* is listed only for those levels below 1715 keV, since it is not known to be different than *I* for levels of higher energies.

TABLE II. Summary of the results of the  $\gamma$ - $\gamma$  coincidence experiments for  $^{156}\text{Eu}$ . All entries in the table are given relative to the particular coincidence spectrum for which they appear, and the code for the entries is given as follows: VS is very strong, S is strong, W is weak, VW is very weak, P is probable, blank is not observed.

$E_{\gamma}$ (keV) \ Gate (keV)	88.95	199.19	317.30	434.40	472.70	490.34	498.88	599.47	646.29	709.86 <sup>a</sup>	723.47	784.14	797.73	811.77	820.36	836.52	841.16 <sup>a</sup>	867.01 <sup>a</sup>	872.39	903.62	928.83	944.35	947.15	960.50 <sup>a</sup>	969.83	1011.87	1037.43
88.95		VS	VW	S	W	W	S	VS	VS	VS*	VS	P	VS	VS	W	P	S*	VS*	W	P	P	VS	S	VS*	S	S	W
190.16									W																		
199.19	W													S		W	VS*	VS*			P		S		VS	S	
317.30										S																	
434.40																											
472.70						S																					
490.34					S																						
498.88																											
585.90			P																								
599.47	S																										
632.79			P																								
646.29	VS																										
707.1																											
709.86	W	W																									
723.47	S																										
768.56		W																									W
784.14																											
797.73																											
811.77	VS	S																	S*							W	
820.36																											
836.52			P														P										
839.0	W																										
841.16	W	S														P					P						
858.36																											
865.98		S												W													
867.01	S																										
872.39																											
903.62																											
916.4																									W		
928.83			P																								
944.35	W																									S	
947.15		S																									
960.50	S																										
961.0																											
969.83		S																					S			S	
1011.87		S																								S	
1018.50																											
1027.39																											
1037.43																											
1040.44																W	VW*				P						
1065.14	VS													VS	W												
1075.99		W															S										
1079.16	VS											VS															VW
1101.80																											
1115.78																											
1129.47																VW						P					
1140.51		W															S										
1153.47	VS		W		W	S				VS	VS	VW											VS				
1154.09															VS	W											
1155.95																										S	
1164.86																	P								W		S
1169.12																									W		
1220.50																									W		
1230.71	VS		P		W	W		W		VS	W*							VS	S								
1242.42			W		W	S				VS	VS	VS	VW										VS		W*		
1258.03																								VW			S
1277.43	VS							VS							W		W*				P						
1366.41								VS							W		W*				P						
1626.29						W																					
1682.12			S			S																					
1857.42	W																										
1877.03	S																										
1937.70	VS																										
2097.70	VS																										
2116.49	W																										

<sup>a</sup> This spectrum was coincident with a complex peak; the entries with an asterisk for this gate indicate  $\gamma$  rays which are partially or totally in coincidence with the unlisted member(s) of the complex peak.

TABLE II (Continued)

Gate (keV) $E_\gamma$ (keV)	1040.44	1065.14	1079.16 <sup>a</sup>	1129.47	1140.51	1153.47	1154.09	1169.12 <sup>a</sup>	1230.71	1242.42	1277.43	1366.41	1626.29	1682.12	1857.42	1877.03	1937.73 <sup>b</sup>	1946.34	1965.95	2026.65 <sup>b</sup>	2032.51 <sup>c</sup>	2097.70	2116.49	2170.86	2180.91	2186.71	2205.38	
88.95	W	VS	VS*	S	VS	VS	S	VS	VS	VS	VW	W	S	VS	VS		S	VS	S	S	VS	S					S	
190.16	VW																											
199.19			S*	S																								
317.30					P				W																			
434.40														W														
472.70					VW	VW*			W																			
490.34					P				W				S															
498.88														S														
585.90											S	W																
599.47											VS	VS																
632.79									W																			
646.29									VS	W*																		
707.1									W																			
709.86					S	W*			S																			
723.47					VS	S*			VS																			
768.56								VW																				
784.14					P				VW																			
797.73			S																									
811.77		VS			VS*	VS																						
820.36											S	S																
836.52	W			P							W	W																
839.0																												
841.16			S*	S																								
858.36			S																									
865.98																												
867.01									VS																			
872.39		P				P																						
903.62											W	P																
916.4																												
928.83																												
944.35					S	S*			VS																			
947.15								S		VW*																		
960.50					W*	S*																						
961.0					W	S*			S																			
969.83																												
1011.87								S																				
1018.50			S																									
1027.39					W	W*			S																			
1037.43			P																									
1040.44			S*	S				W*																				
1065.14																												
1075.99	S			VW																								
1079.16																												
1101.80			W																									
1115.78									VW																			
1129.47			W*	W																								
1140.51	S			VW																								
1153.47																												
1154.09																												
1155.95																												
1164.86	W			P																								
1169.12																												
1220.50																												
1230.71																												
1242.42																												
1258.03																												
1277.43																												
1366.41																												
1626.29																												
1682.12																												
1857.42																												
1877.03																												
1937.70																												
2097.70																												
2116.49																												

<sup>b</sup> This spectrum shows weak evidence for the 160.2-keV  $\gamma$  ray.<sup>c</sup> This spectrum shows probable evidence for the 138.7-keV  $\gamma$  ray.

Note, we have shown that all of the intensity of the 1065.14-keV  $\gamma$  ray belongs to the transition between the  $I\pi K=2+2$  and  $2+0$  levels. This was determined quantitatively from the data in Figs. 4(a) and 5(b). Thus, the relative singles intensities of the 866.0- and 1154.09-keV  $\gamma$  rays were determined by comparing their intensities to that of the 1065.14-keV  $\gamma$  ray. Their relative intensities listed in Table I have been corrected for

angular correlation effects.

By a similar procedure the intensity of the 1153.47-keV  $\gamma$  ray was determined from the spectra coincident with the 709.86- and 723.47-keV  $\gamma$  rays in Figs. 6(a) and 5(d), respectively. As seen in these two figures, both the 1153.47- and 1242.42-keV transitions depopulate the 1242.42-keV  $1^-$  octupole level. When the values determined here for the relative singles intensities of the 1153.47-

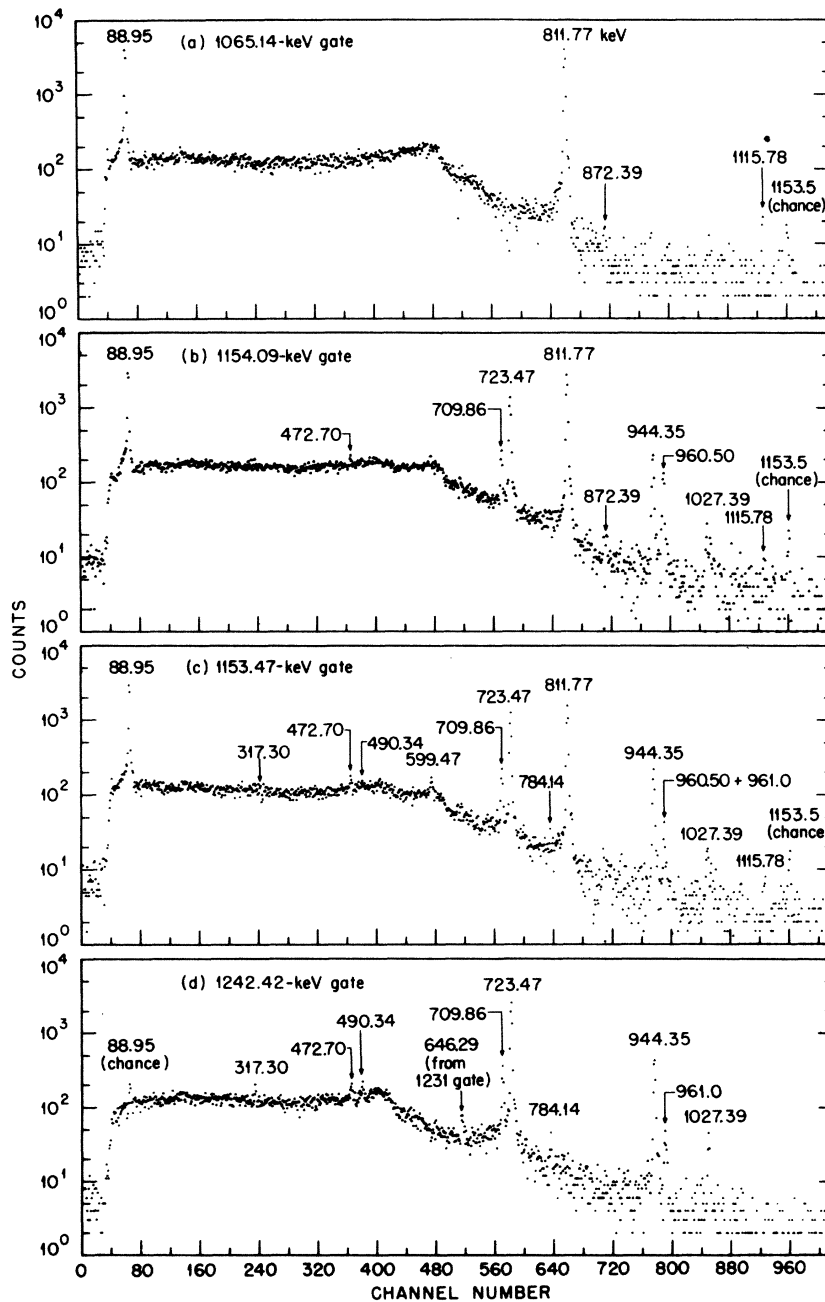


FIG. 4. The  $\gamma$ -ray spectrum of  $^{156}\text{Eu}$  in coincidence with the (a) 1065.14-, (b) 1154.09-, (c) 1153.47-, and (d) 1242.42-keV transitions. These spectra show the transitions which populate the 1154.09 and 1242.42 levels.



and 1154.09-keV transitions are summed, the results agree within error with the relative intensity of the doublet as measured in the singles spectrum. When the doublet peaks such as those at 707.1 and 1037.4 keV were too weak to be resolved from the coincidence experiments, the data in the singles were manually fitted by appropriate Gaussian shapes to determine the relative intensities and energies.

### V. $^{156}\text{Gd}$ LEVEL SCHEME

From the results of the  $\gamma$ -ray singles measurements and the numerous  $\gamma$ - $\gamma$  coincidence experiments, the level scheme of Fig. 3 was constructed. This scheme consists of 26 excited states in  $^{156}\text{Gd}$  and 84 of the 95  $\gamma$ -ray transitions we identify with the decay of  $^{156}\text{Eu}$ . The energy in keV of each transition is given at the top of the arrow representing it and the relative intensities are listed in parentheses. The level energies are weighted averages of the cascade sums and ground state transitions and the assigned errors represent weighted average errors.

Transitions which were shown by the coincidence data to populate an excited level are indicated by a dot at the tip of the arrow, while those which were observed in a coincidence relationship as transitions which deexcite a level are indicated by a dot at the top of the arrow. The spin ( $I$ ) and parity ( $\pi$ ) of each level is listed in the left column; the quantum number  $K$  is listed only for those

levels below 1715 keV, since it is not known to be different than  $I$  for levels of higher energies.

The  $\log ft$  values and internal-conversion coefficients ( $\alpha_K$ ) have been used to infer the spins and parities of the excited states of  $^{156}\text{Gd}$ . The  $\beta^-$  and internal-conversion spectra for  $^{156}\text{Eu}$  decay have been measured by Ewan *et al.*<sup>8</sup> and Peek *et al.*,<sup>9</sup> and they have reported the relative intensities of the conversion lines of the more prominent peaks. By considering the  $\gamma$ -ray and internal-conversion electron intensity balances for a particular level, the  $\beta^-$  branching to that level can be calculated. The direct feeding to the  $0^+$  ground state of  $^{156}\text{Gd}$  was assumed to be 31% which is an average of the values reported by Ewan *et al.*<sup>8</sup> (33%) and Peek *et al.*<sup>9</sup> (29.5%). From the relative  $\gamma$ -ray intensities of Table I and the internal-conversion coefficients of Hager and Seltzer,<sup>27</sup> the percentage  $\beta^-$  branching to each excited state of  $^{156}\text{Gd}$  was calculated. From these percentages,  $\log ft$  values for each  $\beta^-$  branch were calculated with the aid of a computer code.<sup>28</sup> The results are listed in column 4 of Table III along with the percentage branching to each level in column 3. The errors on the entries in column 3 result from the statistical error of the  $\gamma$ -ray intensity balance.

By the normalized  $K$ -conversion peak-to- $\gamma$  peak (NPG) method,<sup>29</sup> the  $K$ -conversion coefficients for the most intense transitions of  $^{156}\text{Gd}$  were determined and are listed in column 3 of Table IV. They were calculated from the  $\gamma$ -ray intensities of Table I and a weighted average of

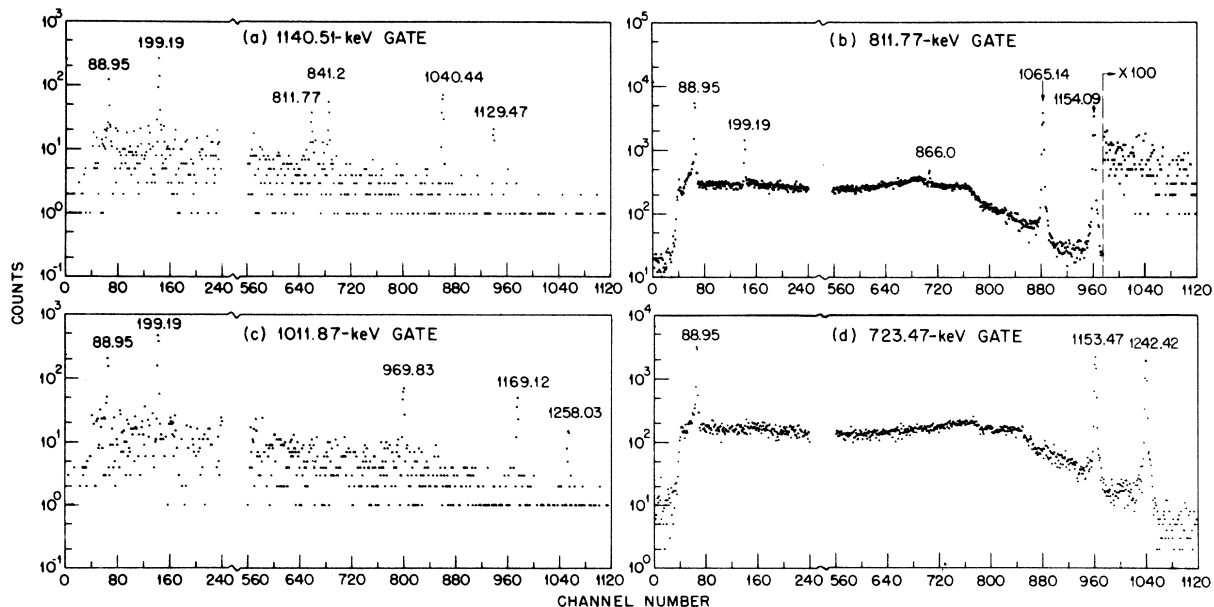


FIG. 5. The  $\gamma$ -ray spectrum of  $^{156}\text{Eu}$  in coincidence with the (a) 1140.51-, (b) 811.77-, (c) 1011.87-, and (d) 723.47-keV transitions. These spectra show the  $\gamma$  rays that depopulate the 1129.41-, 1154.09-, 1258.03-, and 1242.42-keV levels, respectively.

the  $K$ -electron intensities reported by Ewan *et al.*<sup>8</sup> and Peek *et al.*<sup>9</sup> The  $\gamma$ -ray and  $K$ -electron intensities were normalized by assuming that the 960.50- and 1079.16-keV  $\gamma$  rays are  $0^+$  to  $2^+$  transitions as reported by Ewan and Bower<sup>10</sup> and Neilsen, Rud, and Wilsky,<sup>30</sup> respectively, and that both are  $E2$  multipolarity. The 1242.42- and 1366.41-keV  $\gamma$  rays were assumed to be pure  $E1$  transitions.<sup>31</sup> In each case, the theoretical value given by Hager and Seltzer<sup>27</sup> was taken as the  $K$ -conversion coefficient of the pure  $E1$  or  $E2$  transition. The  $\alpha_K$  values were then determined from the equation

$\alpha_K = RI_{eK}/I_\gamma$ , where  $R$  is the average normalizing factor derived from the pure  $E1$  and  $E2$  transitions mentioned above and  $I_{eK}$  is the relative  $K$ -electron intensity for the transition whose relative  $\gamma$ -ray intensity is  $I_\gamma$ . In columns 6, 7, and 8, the theoretical values of Hager and Seltzer<sup>27</sup> for  $E1$ ,  $E2$ , and  $M1$  multipolarity, respectively, are listed for the transitions with energies of 1366.41 keV or less. Above 1366.41 keV, the values of Sliv and Band<sup>32</sup> are given because these energies are beyond the range of the Hager and Seltzer tables. In column 9, the adopted multipolarity is listed.

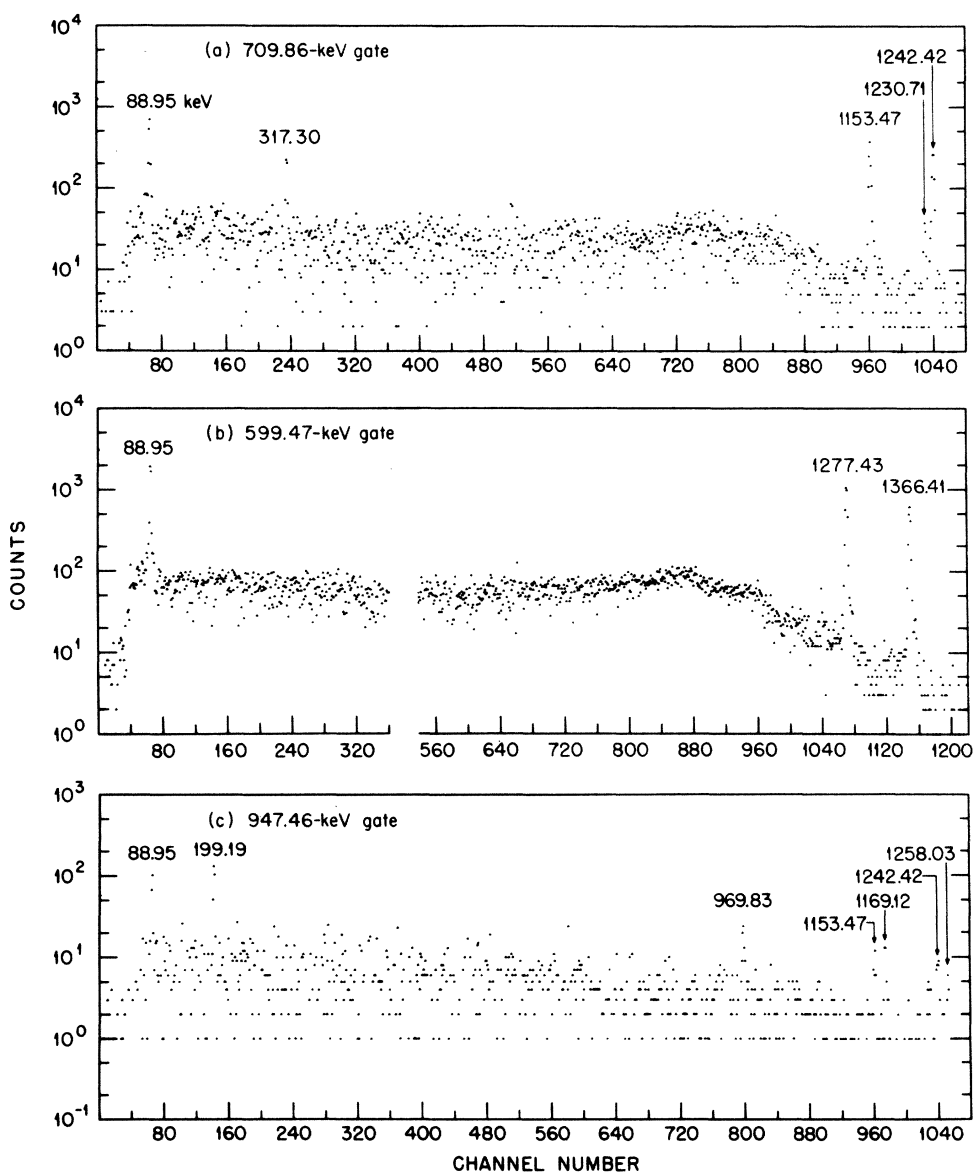


FIG. 6. The  $\gamma$ -ray spectrum of  $^{156}\text{Eu}$  in coincidence with the (a) 709.86-, (b) 599.47-, and (c) 947.46-keV transitions. These spectra show evidence for the levels at 1952.32, 1965.89, and 2205.45 keV. Note that the 947.46-keV gate also includes some of the 944.35-keV  $\gamma$  rays which accounts for the presence of the 1153- and 1242-keV peaks in spectrum (c).

## A. Ground-state band

The  $2^+$  and  $4^+$  members of the ground-state rotational band are well known and the transitions coincident with the 88.95- and 199.19-keV transitions which deexcite these levels were important in the establishment of many of the other levels in  $^{156}\text{Gd}$ .

B.  $0^+$  and  $2^+$  members of the  $\beta$ -vibrational band

The levels at 1049.45 and 1129.41 keV have been reported<sup>8, 17, 22, 25</sup> previously as the  $0^+$  and  $2^+$  members of the  $\beta$ -vibrational band. The earlier  $0^+$  spin-parity assignment<sup>9, 17, 22, 25</sup> is supported by the  $\log ft$  values in Table III, by the  $\alpha_K$  value of the 960.50-keV  $E2$  transition (Table IV) and by

TABLE III.  $\log ft$  values for  $\beta^-$  decay of  $^{156}\text{Eu}$ .

Energy level (keV)	$I\pi K^{a,b}$	Percentage feeding <sup>c</sup>	$\log ft$ value <sup>d</sup>
0	0+0	31.0 ± 2.1	9.8
88.95 ± 0.05	2+0	0.2 ± 4.8	
288.14 ± 0.07	4+0	0.14 ± 0.15	
1049.45 ± 0.09	0+0	1.44 ± 0.15	10.2
1129.41 ± 0.05	2+0	0.084 ± 0.084	
1154.09 ± 0.07	2+2	0.17 ± 0.79	
1168.11 ± 0.07	0+0	4.27 ± 0.28	9.6
1242.42 ± 0.05	1-0	6.1 ± 0.9	9.3
1258.03 ± 0.04	2+0	0.013 ± 0.13	
1319.66 ± 0.08	2-1	0.52 ± 0.61	
1366.40 ± 0.04	1-1	2.53 ± 0.23	9.5
1715.15 ± 0.07	(0+, 1±)	0.001 ± 0.02	
1771.05 ± 0.13	1±	0.004 ± 0.26	
1946.36 ± 0.07	1±	0.47 ± 0.02	9.1
1952.32 ± 0.05	1-	1.02 ± 0.06	8.7
1965.89 ± 0.03	1+	33.2 ± 0.8	7.1
2026.60 ± 0.04	1+	6.3 ± 0.2	7.7
2121.44 ± 0.12	1±	0.13 ± 0.01	9.0
2186.71 ± 0.04	1+	11.6 ± 0.4	6.7
2203.4 ± 0.6	0+, 1±	0.17 ± 0.03	8.4
2205.45 ± 0.05	1±	2.54 ± 0.14	7.2
2259.81 ± 0.17	1±	0.084 ± 0.006	8.3
2269.86 ± 0.04	1+	4.86 ± 0.15	6.5
2293.43 ± 0.11	(1±)	0.091 ± 0.010	8.0
2300.85 ± 0.11	1±	0.114 ± 0.007	7.8
2344.4 ± 0.4	1±	0.010 ± 0.001	8.2
2361.2 ± 0.3	1±	0.021 ± 0.002	7.6

<sup>a</sup> The spins shown here are the best values deduced from all available data, including the  $\log ft$  values of column 4. Values in parentheses are assigned with less certainty than the others.

<sup>b</sup> For the energy levels above 1366.40 keV, the value of  $K$  was assumed to be the same as  $I$ .

<sup>c</sup> The 31%  $\beta^-$  branch to the ground state is an average of the amounts reported by Peek *et al.* (Ref. 9) and Ewan *et al.* (Ref. 8). A total of 0.24% of the  $\gamma$  intensity is unaccounted for.

<sup>d</sup> When the error limits indicated the  $\beta$ -ray feeding could be zero, no  $\log ft$  was calculated.

the absence of  $\gamma$ -ray branching to the  $0^+$  and  $4^+$  levels.

Similarly, our data confirm the spin of the 1129.41-keV level as  $2^+$ . The 1040.44-keV cascade transition from the latter level is reported<sup>11</sup> as 97%  $E2$  from  $\gamma$ - $\gamma(\theta)$  studies, but its  $\alpha_K$  is 6 times larger than the theoretical<sup>27</sup>  $E2$  value. The large  $\alpha_K$  arises from a large  $E0$  admixture in this transition, as was also found<sup>1,7</sup> for the  $2^+ \rightarrow 2^+$  transitions in  $^{152}\text{Sm}$  and  $^{154}\text{Gd}$ .

C.  $0^+$  and  $2^+$  members of a second  $K^\pi = 0^+$  band

Our data confirm the  $0^+$  and  $2^+$  members of the previously reported<sup>9, 14, 17-21, 30</sup>  $K^\pi = 0^+$  band originating at 1168.11 keV. For normalization purposes the  $\alpha_K$  of the 1079.16-keV transition ( $0^+ \rightarrow 2^+$ ) was assumed to be pure  $E2$  multipolarity in order to determine the other conversion coefficients. Alternatively, if the 960.50-keV ( $E2$ ) and 1242.42-keV ( $E1$ ) transitions are used to normalize the relative electron and  $\gamma$ -ray intensities, the 1079.16-keV transition is shown to be pure  $E2$ .

D.  $2^+$   $\gamma$ -vibrational state

From our singles and coincidence data, only the  $2^+$  member of the  $\gamma$ -vibrational band at (1154.09 ± 0.07 keV) is found to be populated in the decay of  $0^+$   $^{156}\text{Eu}$ . Our experimental  $\alpha_K$  values support this  $2^+$  assignment. For the 1065.14-keV transition,  $\alpha_K$  is  $(23.6 \pm 1.8) \times 10^{-4}$  which is slightly larger than the theoretical value<sup>27</sup> of  $20.4 \times 10^{-4}$ . Directional correlation results<sup>11</sup> show that the  $\gamma$ -ray transition is essentially pure  $E2$ ; therefore, the larger conversion coefficient may result from a small amount of  $E0$  admixture.

A search was made for the 959.9- and 1159.1-keV transitions which depopulate the  $3^+$  member of the  $\gamma$  band reported<sup>18</sup> at 1248.09 keV, but no evidence for them was found in the singles or in coincidence data. Upper limits on the relative intensities of these  $\gamma$  rays can be set at about 0.1 units.

## E. Octupole levels

A series of negative parity levels is expected in deformed nuclei for collective octupole oscillations. We see three such levels strongly populated at 1242.42 ± 0.05, 1319.66 ± 0.04, and 1366.40 ± 0.05 keV. In previous measurements<sup>8, 9, 11, 17, 18</sup> these three levels have been assigned spins of  $1^-$ ,  $2^-$ , and  $1^-$ , respectively. Our coincidence data and  $\alpha_K$  values are in complete agreement with these assignments. In addition our data establish numerous new transitions associated with the population and decay of these three levels. It is possible that our unplaced 494.90- and 1187.3-keV transitions populate and depopulate the known<sup>18, 21</sup>

3<sup>-</sup> level as has been suggested by Siddiqi, Cranston, and White.<sup>17</sup> Arguments for the *K*-quantum number assignments are discussed in Sec. VI.

F. High-energy levels previously reported  
in <sup>156</sup>Eu decay

None of the energy levels above 1366.40 keV which are observed from the decay of <sup>156</sup>Eu are reported<sup>18</sup> in the decay of <sup>156</sup>Tb whose ground state is 3<sup>-</sup>, and whose *Q* value for electron capture is 2400 keV.<sup>31</sup> Levels in <sup>156</sup>Gd with spins of 2, 3, or 4 are populated from the decay of <sup>156</sup>Tb by allowed or first forbidden nonunique transitions,

while only states of spin 0 or 1 are populated from the <sup>156</sup>Eu decay by allowed or first forbidden transitions (or a state of 2<sup>-</sup> by unique first forbidden decay). Since spin 2<sup>-</sup> levels of <sup>156</sup>Gd would be populated by allowed <sup>156</sup>Tb decay, and no 2<sup>-</sup> or 2<sup>+</sup> levels are observed above 1370 keV in that decay,<sup>18</sup> none of these higher levels seen from the <sup>156</sup>Eu decay are assigned a spin greater than 1 (it is known that *M2* transitions do not compete favorably with *E1* or *E2* transitions). Admittedly, this is only a weak argument since some <sup>156</sup>Gd level configurations could be such as to prohibit direct electron capture feeding from <sup>156</sup>Tb. Note that with only four exceptions all the higher levels have

TABLE IV. *K*-shell internal-conversion coefficients for <sup>156</sup>Gd transitions.

$E_\gamma$ (keV)	$I_i\pi_i \rightarrow I_f\pi_f$	Experimental $\alpha_K \times 10^4$			Theoretical <sup>a</sup> $\alpha_K \times 10^4$			Adopted multipolarity
		Present work <sup>b</sup>	Ewan <i>et al.</i> <sup>c</sup>	Peek <i>et al.</i> <sup>d</sup>	<i>E1</i>	<i>E2</i>	<i>M1</i>	
88.95	2+ → 0+	14 340 ± 1360	14 000		3370	15 800	24 300	<i>E2</i>
199.19	4+ → 2+	1340 ± 104	1400		390	1580	2490	<i>E2</i>
585.90	1- → 1-	144 ± 90	33		28.4	76.7	147	<i>M1/E2</i>
599.47	1+ → 1-	25.4 ± 2.0	33	35 ± 11	27.1	72.6	139.0	<i>E1</i> <sup>e</sup>
646.29	1+ → 2-	23.6 ± 1.8	24		23.1	60.7	115.0	<i>E1</i> <sup>e</sup>
709.86	1- → 1-	97 ± 8			19.0	48.8	91.1	<i>M1</i>
723.47	1+ → 1-	19.6 ± 1.5		15 ± 2	18.3	46.8	87.0	<i>E1</i> <sup>e</sup>
797.73	1+ → 0+	57 ± 12			15.0	37.6	68.5	<i>M1/E2</i>
811.77	1+ → 2+	67.4 ± 5.0	69		14.5	36.2	65.6	<i>M1</i> <sup>e</sup>
865.99	2+ → 4+	37.4 ± 7.0			12.8	31.5	51.6	<i>E2</i>
858.36	1+ → 1+	78 ± 48			13.0	32.1	57.3	<i>M1/E2</i>
867.01	1+ → 2-	15.0 ± 1.9	13		12.8	31.4	50.6	<i>E1</i>
960.50	0+ → 2+	24.8 ± 2.2	12	12 ± 5	10.5	25.3	43.8	<i>E2</i> <sup>e</sup>
1011.87	1+ → 2+	43 ± 5			9.53	22.7	38.7	<i>M1</i>
1018.50	1+ → 0+	60 ± 12			9.41	22.4	38.1	<i>M1</i>
1040.44	2+ → 2+	126 ± 10			9.04	21.4	36.2	<i>E0/E2</i> <sup>e</sup>
1065.14	2+ → 2+	23.6 ± 1.8	18	26 ± 9	8.66	20.4	34.2	<i>E0/E2</i> <sup>e,f</sup>
1079.16	0+ → 2+	20.1 ± 1.6		16 ± 4	8.46	19.9	33.2	<i>E2</i>
1153.47	1- → 2+	6.9 ± 0.7	8.1	5.3 ± 1.3	7.49	17.4	28.4	<i>E1</i> <sup>e</sup>
1154.09	2+ → 0+	18.4 ± 1.8	16		7.48	17.4	28.3	<i>E2</i>
1230.71	2- → 2+	6.2 ± 0.5	5.7	4.9 ± 0.8	6.67	15.3	24.3	<i>E1</i> <sup>e</sup>
1242.42	1- → 0+	6.3 ± 0.5	7.5		6.56	15.0	23.8	<i>E1</i>
1277.43	1- → 2+	5.6 ± 0.5			6.24	14.2	22.3	<i>E1</i>
1366.41	1- → 0+	5.5 ± 0.7	5.3		5.55	12.5	19.1	<i>E1</i>
1877.03	1+ → 2+	10.7 ± 1.2	6.4	6.7 ± 1.1	3.29	6.91	9.08	<i>M1/E2</i> <sup>e</sup>
1937.71	1+ → 2+	9.3 ± 0.9	6.6		3.12	6.52	8.45	<i>M1/E2</i> <sup>e</sup>
1965.95	1+ → 0+	9.3 ± 0.7	7.2		3.05	6.35	8.19	<i>M1</i>
2026.65	1+ → 0+	7.9 ± 0.7	7.6	10 ± 8	2.91	6.00	7.65	<i>M1</i>
2097.70	1+ → 2+	7.4 ± 0.6	6.7	6.6 ± 0.8	2.75	5.64	7.08	<i>M1/E2</i> <sup>e</sup>
2180.91	1+ → 2+	6.2 ± 0.6	5.6	7.9 ± 3.2	2.59	5.26	6.49	<i>M1/E2</i>
2186.71	1+ → 0+	8.1 ± 0.6		7.6 ± 1.4	2.58	5.23	6.45	<i>M1</i>

<sup>a</sup> Values taken from Hager and Seltzer (Ref. 27) for transitions ≤ 1366.41 keV; for transitions of 1877.03 keV and above, values from Sliv and Band (Ref. 32) were used.

<sup>b</sup> Calculated using our  $\gamma$ -ray intensities and a weighted average of the *K*-electron intensities of Ewan *et al.* (Ref. 8) and Peek *et al.* (Ref. 9).

<sup>c</sup> From Ref. 8.

<sup>d</sup> From Ref. 9.

<sup>e</sup> The multipolarity of these  $\gamma$ -ray transitions has been determined in directional correlation measurements of Hamilton *et al.* (Ref. 11).

<sup>f</sup> Reference 11 reports this transition to be 97.7% quadrupole radiation; therefore, the conversion coefficient can only be explained by an *E0* admixture of at least 5%.

about equal ratios of decay intensity to the ground and  $2^+$  levels.

1.  $1771.05 \pm 0.13$ -keV level  $1^+$

A level at 1771.05 keV is established in the  $^{156}\text{Eu}$  decay from the spectra coincident with the 434.40- and the 1682.12-keV transitions. The level was reported previously in neutron capture studies.<sup>13-15, 17</sup> No evidence is observed for depopulating transitions other than the 1682.12-keV  $\gamma$  ray to the  $2^+$  level. From the relative strengths of the primary  $E1$  and  $M1$  transitions following neutron capture,<sup>15</sup> the spin-parity is limited to  $1^+$  or  $2^+$ . Since this state is not observed in  $^{156}\text{Tb}$  decay,<sup>18</sup> its spin-parity assignment is probably  $1^+$ .

2.  $1965.89 \pm 0.02$ -keV level  $1^+$

The spin of the 1965.89-keV level has been shown to be  $1^+$  from directional correlation results<sup>11</sup> and from the  $\alpha_K$  values listed in Table IV for the strong transitions which depopulate it. No  $\gamma$ -ray population of the 1965.89-keV level was observed, so direct feeding from  $\beta^-$  decay of  $^{156}\text{Eu}$  is the primary means of population.

Siddiqi *et al.*<sup>17</sup> report a 1965.91-keV level and assign it a spin of  $3^-$ . This level is presumably the same one we see since there is agreement on the three strongest deexciting transitions. The 1965.95-keV ground-state transition was masked in their work by another strong transition of about the same energy. Further, their 957.94-keV transition to a  $5^-$  level is definitely not seen in our work; so it does not depopulate this level. However, our coincidence data show the 646.29-keV transition definitely depopulates this level and little if any of its intensity belongs to an alternate placement<sup>17</sup> out of a 2054-keV level. Less than 1.5 units of the intensity we assign to the 1965.95-keV  $\gamma$  ray can belong to their primary transition of this energy originating at a 2054-keV level.

3.  $2026.60 \pm 0.04$ -keV level  $1^+$

Earlier, a  $1^+$  level was placed<sup>31</sup> near 2026.60 keV with decay<sup>8</sup> to the  $0^+_g$ ,  $2^+_g$ , and 1168.11-keV levels. Our coincidence data confirm these three transitions and reveal new transitions of 784.14, 768.56, and 707.1 keV which deexcite this level and a 160.2-keV  $\gamma$  ray which feeds it. Directional correlation measurements<sup>11</sup> yield a spin of 1 for the 2026.60-keV state and give a 75.5% dipole admixture for the 1937.73-keV transition. Even parity is established by the  $\alpha_K$  values of the 1937.73- and 2026.65-keV transitions. Our data show the 1738.9-keV transition of Siddiqi *et al.*<sup>17</sup> does not

depopulate this level and does presumably belong to their alternate placement out of a level at 1827.9 keV.

4.  $2186.71 \pm 0.04$ -keV level  $1^+$

The previously reported<sup>31</sup> level near 2186.71 keV is confirmed by our experiments. Based on the  $\alpha_K$  values in Table IV and angular correlation results<sup>11</sup> a spin-parity assignment of  $1^+$  is made.

5.  $2203.4 \pm 0.6$ -keV level  $0^+, 1^+$

Some confusion has existed concerning levels at about this energy. At first a single level was reported<sup>8</sup> at 2203 keV and later at 2205 keV<sup>16</sup> with both based on the same decaying transition. Two levels were suggested tentatively and dashed in at 2202.5 and 2203.2 keV by Peek *et al.*<sup>9</sup> In an abstract Ewan and Bower<sup>10</sup> mention a new level at 2205 keV. Our coincidence data clearly show that there are two close lying levels and the lower of these is at 2203.4 keV. The  $\log ft$  of 8.4 to this level and the absence of population in the  $^{156}\text{Tb}$  decay indicate the spin-parity assignments of  $0^+$ ,  $1^\pm$ . A negative parity level is reported<sup>15</sup> at  $2203.5 \pm 1.5$  keV in  $(n, \gamma)$  studies, but the data do not allow us to conclude whether this is either the 2203.4- or 2205.45-keV level seen from our measurements.

6.  $2205.45 \pm 0.05$ -keV level  $1^+$

This is a level that was tentatively suggested<sup>10</sup> earlier. It is well established in the present work both by several coincidence gates and by the 2205.38-keV ground-state transition. A 1049.4-keV transition seen in electron work<sup>16</sup> was incorrectly placed<sup>31</sup> between 2205- and 1154-keV levels. It results from the  $E0$  decay of the 1049.45-keV  $0^+$  level.<sup>10</sup> The other  $\gamma$  rays that deexcite this level as cascade transitions are all observed in the present coincidence data and firmly establish this level. Since the state decays directly to  $0^+$  and  $2^+$  levels, assignments of  $0^\pm$  and  $2^-$  are eliminated. The  $\log ft$  value for  $\beta$ -ray feeding is 7.2 in agreement with an allowed or a first forbidden nonunique transition. Thus,  $I^\pi$  is  $1^+$  or  $1^-$ .

7.  $2269.86 \pm 0.04$ -keV level  $1^+$

This is another level which was tentatively assigned<sup>10</sup> earlier. It is now well established by our coincidence data which placed six new deexciting transitions. The 2269.90-keV transition to the  $0^+$  ground state eliminates assignments of  $0^\pm$  and  $2^-$ , the  $\log ft$  of 6.5 eliminates its spin as  $2^+$ , and the  $\alpha_K$  for the 2180.91-keV transition to the  $2^+$  state

agrees with  $M1/E2$  multipolarity indicating even parity. So  $I^\pi$  is  $1^+$ .

#### G. Energy levels placed for the first time

Several new energy levels were placed in the level scheme from energy sum relationships and from coincidence relationships or both. When using energy sum relationships alone, our criterion was that the sum of the energies of various cascades and ground state transitions from a level must agree within 0.3 keV. From the coincidence data, a single confirmed coincidence relationship was assumed to be adequate to establish a new level.

##### 1. $1715.15 \pm 0.07$ -keV level ( $0^+, 1^+$ )

The 1715.15-keV level is based on the numerous transitions coincident with the 490.34- and 472.70-keV  $\gamma$  rays. There is no evidence for  $\beta^-$  feeding to this level. Its decay to  $2^+$  states eliminates a spin-parity assignment of  $0^-$ . Since a level of this energy is not observed<sup>18</sup> in the decay of  $^{156}\text{Tb}$ , the tentative spin assignment is  $0^+$  or  $1^+$ .

##### 2. $1946.36 \pm 0.07$ -keV level $1^+$

Our placement of this level is based on the observation of a 1946.34-keV ground-state transition and a 1857.42-88.95-keV coincident  $\gamma$ -ray cascade. The 1857.42-keV transition is 99.94% dipole and is the first member of 1-2-0 cascade determined from  $\gamma$ - $\gamma(\theta)$  work.<sup>11</sup> Thus,  $I^\pi$  is  $1^+$ .

Apparently this level is not the same as that placed at 1945.87 keV by Siddiqi *et al.*<sup>17</sup> They show a quite different pattern of branching from their level and make a tentative spin assignment of  $2^+$ . It is true that they see  $\gamma$  rays with both the same energies and relative intensities as the two transitions we place from the 1946.36-keV level. But in addition they show other strong deexciting transitions which simply do not appear in our data. Thus, one might conclude that there are two very close lying levels populated in the ( $n, \gamma$ ) work.

##### 3. $1952.32 \pm 0.05$ -keV level $1^-$

This level was placed on the basis of the coincidence data [e.g., see Fig. 6(a)] which show that it decays to the three negative parity octupole levels. Since this state deexcites by a 709.86-keV  $M1$  transition (see Table IV) to the  $1^-$ , 1242.42-keV level and by a transition to a  $2^-$  state, the  $I^\pi$  choices are restricted to  $1^-$  and  $2^-$ . The fact that it is not populated by allowed electron capture from  $^{156}\text{Tb}$  further suggests the choice of  $1^-$ .

##### 4. $2121.44 \pm 0.12$ -keV level $1^+$

Our observation of a 2032.51-88.95-keV coincident cascade and a  $2121.3 \pm 0.4$ -keV crossover transition are the basis for this level assignment. These data, coupled with a  $\log ft$  value of 9.0, restrict  $I^\pi$  to  $1^+$ .

##### 5. $2259.81 \pm 0.17$ -keV level $1^+$

A ground-state transition plus a coincident cascade to the 88.95- and the 2121.44-keV levels dictate this level assignment. Again, these data along with the  $\log ft$  value indicate  $I^\pi = 1^+$ .

##### 6. $2293.43 \pm 0.11$ -keV level $1^+$

Observation of the 1164.2-keV  $\gamma$  ray in the spectrum coincident with the 841.16- and 1040.44-keV  $\gamma$  rays establishes this level. In addition, the spectrum coincident with 1164.2-keV  $\gamma$  rays shows 841.16-, 1040.44-, and 1129.47-keV transitions to confirm that the 1164.2-keV  $\gamma$  ray populates the 1129.41-keV level. The  $2293.40 \pm 0.12$ -keV  $\gamma$  ray fits well as a ground-state transition and therefore would eliminate  $I^\pi$  assignments of  $0^+$  and  $2^-$ . The  $\log ft$  value of 8.0 eliminates  $2^+$  to yield  $1^+$ .

At this point we find a possible disagreement with Siddiqi *et al.*<sup>17</sup> who report a 2293.2-keV transition along with 1106.0- and 974.33-keV ones which they suggest depopulate a 2382.2-keV ( $3^-$ ) level. We could not see their other two  $\gamma$  rays which are weaker than the 2293.2-keV transition, but they should have seen an 1164.2-keV  $\gamma$  ray if our 2293.40-keV transition is the same as that in their work. Tentatively, we conclude that these two observations of levels at about 2293 keV result from different levels.

##### 7. $2300.85 \pm 0.11$ -keV level $1^+$ and $2344.4 \pm 0.4$ -keV level $1^+$

These two levels are placed in the decay scheme from energy sum relationships only. The energy difference of 89.2 keV between the 2301.0- and 2211.8-keV  $\gamma$  rays suggests that they populate the ground and first  $2^+$  states, respectively. Similarly, the energy difference of 88.8 keV between the 2344.3- and 2255.5-keV  $\gamma$  rays suggests the same decay pattern. No conclusive information was obtained from the coincidence data on these weak high-energy peaks. The  $\log ft$  values of 7.8 and 8.2, respectively, for  $\beta^-$  decay to the 2300.85- and 2344.1-keV levels and the apparent ground-state transitions from each restrict  $I^\pi$  to  $1^+$  in each case.

Siddiqi *et al.*<sup>17</sup> proposed a level at 2300.47 keV from their ( $n, \gamma$ ) studies. They do not see a ground-

TABLE V. Reduced  $B(E1)$  transition probability ratios from octupole levels at 1242.42 and 1366.41 keV in  $^{156}\text{Gd}$ .

Energy level (keV)	$\frac{B(E1;K_i I_i \rightarrow K_f I_f)}{B(E1;K_i I_i \rightarrow K_f I_f')}$	$\frac{E(I_i \rightarrow I_f)}{E(I_i \rightarrow I_f')}$	Experimental ratios	Theoretical ratios <sup>a</sup>	
				$K=0$	$K=1$
1242.42	$\frac{B(E1;K1 \rightarrow 00)}{B(E1;K1 \rightarrow 02)}$	$\frac{1242.42}{1153.47}$	0.81 ± 0.09	0.5	2.0
1366.40	$\frac{B(E1;K1 \rightarrow 00)}{B(E1;K1 \rightarrow 02)}$	$\frac{1366.41}{1277.43}$	0.45 ± 0.03	0.5	2.0

<sup>a</sup> From the predictions of the adiabatic symmetric rotor model.

state transition, but this would have been most difficult due to the complexity of their spectra. After an examination of both sets of data it appears probable that their 2300.47-keV level corresponds to that assigned in the present work, but that three of the four transitions they show depopulating the state actually belong elsewhere. Indeed, there remains the possibility that they observe a distinctly different level of higher spin with nearly the same energy.

#### 8. 2361.2 ± 0.3-keV level $1^\pm$

This highest-energy level observed in  $^{156}\text{Gd}$  is placed on the basis of a 2361.2-keV  $\gamma$  ray observed in the singles spectrum. This transition must decay to the ground state because the  $Q$  value for  $\beta^-$  decay of  $^{156}\text{Eu}$  is  $2430 \pm 10$  keV.<sup>8</sup> The  $\log ft$  of 7.6 and decay to the  $0^+$  ground state again limit  $I^\pi$  to  $1^\pm$ . We could not determine if a 2272.2-keV transition to the  $2_2^+$  level were present since it would be masked by the strong 2269.90 keV  $\gamma$  ray.

Weak  $\gamma$  rays at 335.69, 348.27, 354.20, and 554.66 keV could be placed in this level scheme on the basis of energy fit. However, we chose not to do so because in most cases their low intensity does not provide a clear-cut interpretation in the coincidence data.

The remaining unplaced  $\gamma$  rays have energies of 215.7, 244.7, 281.4, 290.49, 494.90, 1187.3, and 2110.52 keV. The sum of the intensities of the unplaced  $\gamma$  rays amounts to 2.14 units or 0.24% of the total  $\beta^-$  decay. These could possibly influence the intensity balances used in the  $\log ft$  assignments of the weakly (~0.24%) populated levels.

## VI. DISCUSSION

The present studies on the  $^{156}\text{Gd}$  levels have clarified numerous cases of conflicting data that existed previously. Further, our measurements have established the properties of many new levels in this nucleus. Thus, for several levels it has

become possible to make meaningful comparisons between experimental results and theoretical predictions.

Recently we<sup>26</sup> applied a second-order perturbation treatment to the two excited  $K=0$  bands and the  $\gamma$ -vibrational band in  $^{156}\text{Gd}$  (for details see Ref. 26). In summary, the results were that the inclusion of the second-order effects of mixing between the  $\beta$ - and  $\gamma$ -vibrational bands did not give a consistent set of  $Z_\beta$  values for the three branching ratios from the  $2^+$  state (1129.41 keV) of the so called  $\beta$ -vibrational band. However, this treatment did give a consistent set of  $Z_\gamma$  values for the  $\gamma$ -vibrational band and within just over 1 standard deviation in the error limits, produced consistent  $Z_\beta$  values for the  $2^+$  member of the second excited  $K^\pi = 0^+$  band.

Let us briefly turn to the three negative parity states around 1300 keV which are considered to be members of octupole bands. The 1242.42-keV level with a spin of  $1^-$  has been assigned<sup>18,22</sup> to a  $K^\pi = 0^-$  octupole band, while the 1366.40- and 1319.66-keV levels with spins of  $1^-$  and  $2^-$  tentatively have been assigned<sup>18</sup> to the  $K^\pi = 1^-$  octupole band. We have computed the  $B(E1)$  ratios for the two  $I^\pi = 1^-$  levels and compared them with rotational predictions. As seen in columns 5 and 6 of Table V, there is obviously poor agreement between experiment and theory for the 1242.42-keV level and also for the 1366.40-keV level if the previous  $K=1$  assignments are correct.

It is well known that the effects of Coriolis coupling play an important role in the properties of the octupole states. Neergård and Vogel<sup>33</sup> and Kocbach and Vogel<sup>34</sup> have demonstrated this for several deformed nuclei with calculations which include the random phase approximation with Coriolis coupling. The interaction is apparent in that levels of equivalent odd spins for the  $K^\pi = 0^-$  and  $1^-$  bands are displaced away from one another. As has been observed<sup>3,7</sup> in  $^{154}\text{Gd}$ , we see in  $^{156}\text{Gd}$  that when the band heads are close in energy the effect is greatest. In both of these nuclei the normal spin sequence has been inverted

to  $I = 2, 1, 3$ , etc. Thus, it is possible that the Coriolis coupling accounts for much of the difference between the experimental  $B(E1)$  ratios and the predictions of the adiabatic symmetric rotor model.

The authors are grateful to R. J. Silva for his help in the chemical purification of the sources and to A. R. Brosi and B. H. Ketelle for the use of experimental equipment as well as for their help in some of the measurements.

\*Oak Ridge Graduate Fellow from Vanderbilt University under appointment from Oak Ridge Associated Universities. Present address: U. S. Atomic Energy Commission, Washington, D. C.

†Research sponsored by the U. S. Atomic Energy Commission under contract with Union Carbide Corporation.

‡Work supported in part by a grant from the National Science Foundation.

- <sup>1</sup>L. L. Riedinger, N. R. Johnson, and J. H. Hamilton, Phys. Rev. Lett. **19**, 1243 (1967); Phys. Rev. **179**, 1214 (1969).
- <sup>2</sup>L. Liu, O. B. Nielsen, P. Salling, and O. Skilbreid, Izv. Akad. Nauk SSSR Ser. Fiz. **31**, 63 (1967) [transl.: Bull. Acad. Sci. USSR, Phys. Ser. **31**, 69 (1967)].
- <sup>3</sup>R. A. Meyer, Phys. Rev. **170**, 1089 (1968).
- <sup>4</sup>R. G. Stokstad, J. S. Greenberg, I. A. Fraser, S. H. Sie, and D. A. Bromley, Phys. Rev. Lett. **27**, 748 (1971).
- <sup>5</sup>L. Varnell, J. D. Bowman, and J. Trischuk, Nucl. Phys. **A127**, 270 (1969).
- <sup>6</sup>J. H. Hamilton, A. V. Ramayya, and L. C. Whitlock, Phys. Rev. Lett. **22**, 65 (1969); Phys. Rev. **C 3**, 313 (1971).
- <sup>7</sup>L. L. Riedinger, N. R. Johnson, and J. H. Hamilton, Phys. Rev. **C 2**, 2358 (1970).
- <sup>8</sup>G. T. Ewan, R. L. Graham, and J. S. Geiger, Nucl. Phys. **29**, 153 (1962).
- <sup>9</sup>N. F. Peek, J. A. Jungerman, and C. G. Patten, Phys. Rev. **136**, B330 (1964).
- <sup>10</sup>G. T. Ewan and R. H. J. Bower, Bull. Am. Phys. Soc. **11**, 11 (1966).
- <sup>11</sup>J. H. Hamilton, P. E. Little, A. V. Ramayya, E. Collins, N. R. Johnson, J. J. Pinajian, and A. F. Kluk, Phys. Rev. **C 5**, 899 (1972).
- <sup>12</sup>N. Rud and K. B. Neilsen, Nucl. Phys. **A158**, 546 (1970).
- <sup>13</sup>L. V. Groshev, A. M. Demidov, V. A. Ivanov, V. N. Lutsenko, and K. I. Pelekhov, Izv. Akad. Nauk SSSR Ser. Fiz. **26**, 1119 (1962) [transl.: Bull. Acad. Sci. USSR, Phys. Ser. **26**, 1127 (1962)].
- <sup>14</sup>A. Backlin, B. Fogelberg, G. Hedin, M. Saraceno, R. C. Greenwood, C. W. Reich, H. R. Koch, H. A. Baader, H. D. Breitig, and O. W. B. Schult, in *Proceedings of the International Symposium on Neutron-Capture Gamma-Ray Spectroscopy, Studsvik, Sweden, August 1969* (International Atomic Energy Agency, Vienna, Austria, 1969), p. 147.
- <sup>15</sup>L. M. Bollinger and G. E. Thomas, Phys. Rev. **C 2**, 1951 (1970).
- <sup>16</sup>B. S. Dzhelepov, A. G. Dmitriev, N. N. Zukovskii, and A. G. Maloyan, Izv. Akad. Nauk SSSR Ser. Fiz. **30**, 394 (1966) [transl.: Bull. Acad. Sci. USSR, Phys. Ser. **30**, 401 (1966)].
- <sup>17</sup>T. A. Siddiqi, F. P. Cranston, and D. H. White, Nucl. Phys. **A179**, 609 (1972).
- <sup>18</sup>D. J. McMillan, J. H. Hamilton, and J. J. Pinajian, Phys. Rev. **C 4**, 542 (1971).
- <sup>19</sup>P. F. Kenealy, E. G. Funk, and J. W. Mihelich, Nucl. Phys. **A105**, 522 (1967).
- <sup>20</sup>M. Fujioka, Nucl. Phys. **A153**, 337 (1970).
- <sup>21</sup>J. H. Hamilton, M. Fujioka, J. J. Pinajian, and D. J. McMillan, Phys. Rev. **C 5**, 1800 (1972).
- <sup>22</sup>R. Bloch, B. Elbek, and P. O. Tjøm, Nucl. Phys. **A90**, 576 (1967).
- <sup>23</sup>H. Morinaga, Nucl. Phys. **75**, 385 (1966).
- <sup>24</sup>Y. Yoshizawa, B. Elbek, B. Herskind, and M. C. Olesen, Nucl. Phys. **73**, 278 (1965).
- <sup>25</sup>G. B. Hagemann, L. L. Riedinger, E. Eichler, J. Fuglsang, B. Herskind, and B. Elbek, unpublished; L. L. Riedinger, private communication.
- <sup>26</sup>A. F. Kluk, N. R. Johnson, and J. H. Hamilton, Z. Phys. **253**, 1 (1972).
- <sup>27</sup>R. S. Hager and E. C. Seltzer, Nucl. Data **A4**, 1 (1968).
- <sup>28</sup>J. T. Larsen and R. G. Lanier, Lawrence Radiation Laboratory (to be published).
- <sup>29</sup>B. van Nooijen, in *Internal Conversion Processes*, edited by J. H. Hamilton (Academic, New York, 1966), p. 35.
- <sup>30</sup>H. L. Nielsen, N. Rud, and K. Willsky, Phys. Lett. **30B**, 169 (1969).
- <sup>31</sup>C. M. Lederer, J. M. Hollander, and I. Perlman, *Table of Isotopes* (Wiley, New York, 1968), 6th ed., 314ff.
- <sup>32</sup>L. A. Sliv and I. M. Band, *Alpha-, Beta-, and Gamma-Ray Spectroscopy* (North-Holland, Amsterdam, 1965), p. 1639.
- <sup>33</sup>K. Neergård and P. Vogel, Nucl. Phys. **A145**, 33 (1970).
- <sup>34</sup>L. Kocbach and P. Vogel, Phys. Lett. **32B**, 434 (1970).